Plasma Phys. Control. Fusion **49** (2007) 105–112 doi:10.1088/0741-3335/49/2/001

The lift-off stage of plasma focus discharges

H Bruzzone[1], **H Acuña**[1] **and A Clausse**[2]

[1] Universidad de Mar del Plata and CONICET, 7600 Mar del Plata, Argentina
[2] CNEA-CONICET and Universidad Nacional del Centro, 7000 Tandil, Argentina

Received 18 September 2006, in final form 23 November 2006
Published 3 January 2007
Online at stacks.iop.org/PPCF/49/105

Abstract
A simple model describing the lift-off of the current sheet in the initial stage of plasma focus (PF) discharges is presented. The model results are supported by measurements performed on a low energy PF device and also with other experimental results found in the literature. The ideas used in the model have a sufficient general validity so that they can be applied to essentially all existing PF devices.

1. Introduction

The influence of the current sheet (CS) detachment in the initial stage of plasma focus (PF) discharges on the pinch properties is well documented. In spite of this, the dynamics of this stage is still not well understood. Formation times of the plasma film over the cylindrical insulator surrounding the central electrode have been reported, based on visible light pictures of the CS (Krompholz *et al* 1980, Moreno *et al* 2003) and also on magnetic probe measurements (Oppenlander 1978, Gourlan *et al* 1979, Bruzzone and Grondona 1997), ranging from ≈100 ns up to 1 μs. Such time delay, called the 'lift-off time', is ordinarily determined as the time difference between the start of the discharge current and the time at which the CS starts to move.

A comprehensive theoretical picture of the CS-formation stage should take into account the ionization mechanisms responsible for the transition between a neutral gas and a fully ionized plasma. In principle, there is sufficient available theoretical knowledge to model in detail these processes, but the whole procedure is so cumbersome that simpler lumped models seem advisable and convenient to feed into presently available PF codes (Casanova *et al* 2005, Gonzalez *et al* 2004). The problem arising with simple models is how reliable they can be, an issue which should ultimately be validated against experimental data. Furthermore, usually the initial width of the CS is not predicted by simple models and should be provided separately for each device and operating conditions.

In this work, a simple model describing the lift-off of the CS in the initial stage of PF discharges is presented. The model results are supported by measurements performed on a low energy PF device. The ideas used in the model have, however, sufficient general validity so that they can be applied to essentially all existing PF devices within their operating pressure range of operation, provided that the relevant parameters are measured.

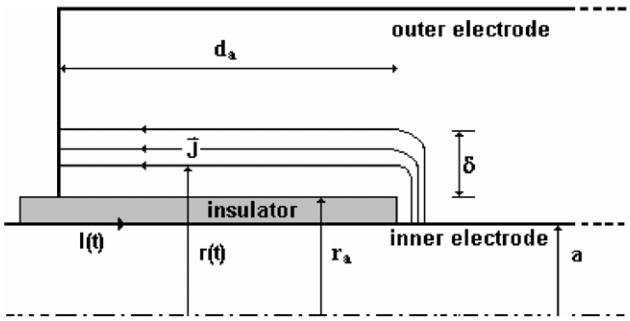

Figure 1. Schematic diagram of the lift-off stage of a PF.

2. Experimental studies

The experiments were done using a PF device whose bank capacity C_0 is 12.6 μF and was charged at $V_0 = 30$ kV; its inductance L_0 (measured with a short circuit on the insulator) is 40 nH (including 1.8 nH of the initial discharge on the insulator), the inner and outer radii (a and b) are 1.8 cm and 3.6 cm, respectively, and their lengths are 10 cm. The radius and length of the insulator (Pyrex glass) are 2.3 cm and 3.6 cm, respectively. The discharge chamber was evacuated down to less than 10^{-5} mbar for several minutes every time the gas was changed and then filled with fresh deuterium gas at the desired pressure. The pressure was measured by means of a capacitive manometer with an effective uncertainty of ± 0.05 mbar. Ten consecutive shots were done with the same gas filling, monitoring the stagnant-pressure changes (if any) from shot to shot. The voltage evolution between electrodes, $V(t)$, was measured with a calibrated fast resistive voltage divider and the time derivative of the discharge current, $\mathrm{d}I/\mathrm{d}t$, with a Rogowski coil. The signals were recorded using 2 ns-resolution digital oscilloscopes. The values of $V(t)$ and $\mathrm{d}I/\mathrm{d}t$ were recorded for 60 shots performed in the above described conditions at 1, 2, 3, 4, 5 and 6 mbar and used to extract from them the time varying gun inductance, $L_\mathrm{p}(t)$, as described in a previous work (Bruzzone *et al* 2006b).

3. Lift-off model

Successfully operating PF devices are known to produce the initial plasma (CS) on the insulator separating the coaxial electrodes at their breach end. Figure 1 shows a diagram of the first instants of a CS lifting off from a cylindrical insulator surrounding the anode front of a coaxial gun, having radius r_a and length d_a.

Assuming that the chamber is filled with deuterium gas, the initial gas atomic density n_0 (m^{-3}) is about 5.4×10^{22} times p_0, p_0 being the filling pressure in mbar.

The first item to address is the gas-plasma conditions in the CS when the current $I(t)$ 'starts' or more appropriately at the time t_0 of the first peak of the $\mathrm{d}I/\mathrm{d}t$, a feature which is more amenable to physical interpretation and can be easily determined in typical Rogowski signals. From transient electrical circuit theory (Bruzzone *et al* 1989), it is known that when the initial peak of $\mathrm{d}I/\mathrm{d}t$ equals V_0/L_0, the total series resistance in the circuit drops well below $\sqrt{L_0/C_0}$. The main component of this resistance is determined by the summation of the (time varying) spark-gap resistance and that in the forming CS, R_CS. Therefore, at t_0 (measured from the start of $\mathrm{d}I/\mathrm{d}t$) one can confidently assume that $R_\mathrm{CS} \leqslant 0.1(L_0/C_0)^{1/2}$. Consequently, assuming a uniform and symmetric CS, the upper bound of its resistivity can be calculated as

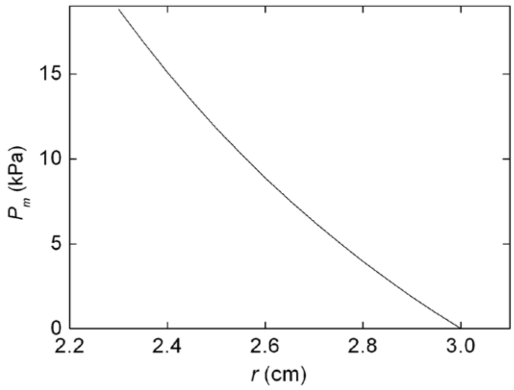

Figure 2. Magnetic pressure inside a 0.7 cm width CS generated by a flowing current of 25 kA at time t_0.

(MKS units are used throughout except where noted)

$$\eta(t_0) \leqslant 0.1\left(\frac{L_0}{C_0}\right)^{1/2} \frac{\pi\left[\left(r_a + \delta\right)^2 - r_a^2\right]}{d_a}. \qquad (1)$$

For example, for the experimental device described in this article, assuming an initial CS width $\delta = 0.4$ cm, one obtains $\eta(t_0) \leqslant 0.002\,\Omega$ m.

On the other hand, in a partially ionized plasma, with electron density $n(t_0) < n_0$, η is approximately given by (MKS units are used throughout except where noted)

$$\eta(t_0) = \frac{m_e}{e^2 n}(\nu_{ei} + \nu_{en}) = \frac{9.17 \times 10^{-32}}{(kT_e)^{3/2}} + 1.51 \times 10^4 \left(\frac{n_0}{n(t_0)} - 1\right)(kT_e)^{1/2}, \qquad (2)$$

where e and m_e are the electron charge and mass, ν_{ei} and ν_{en} are the electron–ion and electron–neutral collision frequencies and a constant value 5×10^{-19} m^2 was chosen for the electron–neutral elastic collision cross section (Huba 2006). Further assuming $T_e \approx 2$ eV, one finds an ionization degree at this instant of time $n(t_0)/n_0 \geqslant 0.006$. This figure agrees with the ionization degree estimated from the energy delivered to the plasma up to t_0, calculated from $V(t)$ and dI/dt signals (Bruzzone and Acuña 2006a). Therefore, it is reasonable to say that at t_0 the plasma in the CS is partially ionized (≈1%) with a sizable resistivity (which in turn supports the uniform current density assumption). In this condition the electron ion thermalization time is about 700 ns, meaning that both ions and atoms are probably still at ambient temperature. The plasma pressure is then about the electron component pressure, which is dominated by the magnetic pressure $P_m = B(r)^2/2\,\mu_0$ generated by the current flowing at t_0.

A plot of P_m within the CS at $t = t_0$ is given in figure 2, for $I(t_0) = 25$ kA and $\delta = 0.4$ cm (typical experimental values at $p_0 = 1$ mbar). The plasma pressure estimated in this condition (1% ionization degree, $T_e \approx 2$ eV) is about 170 N m^{-2}, much smaller than P_m (excluding the outer portion of the CS). Hence, the electron gas will be pushed outwards, carrying along the ions, which in turn would sweep the neutral atoms since the mean free path for charge exchange collisions at 1 mbar is smaller than 0.04 mm (Brown 1967) (i.e. each charge exchange collision transforms a moving ion and a standing atom into a moving atom and a standing ion, which will be dragged by the electrons). The net result is that the magnetic pressure acts on all the mass density in the CS. This picture of the forming CS holds well between 1 and 6 mbar.

To describe the kinematics of this initial structure, a snowplough model is proposed here starting with the following assumptions.

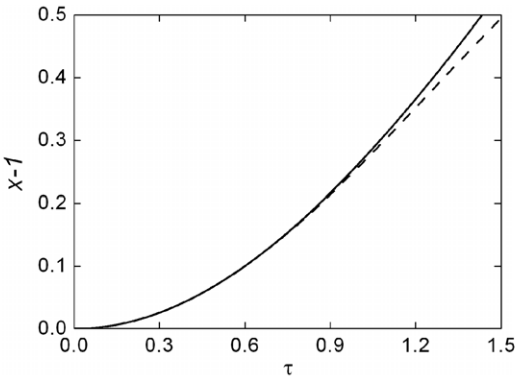

Figure 3. Evolution of the trailing edge of the initial CS. The solid line is the numerical solution of equation (7), the dashed line is the approximate solution given by equation (8).

- The movement is limited to a thin sheet, initially lying on the insulator, which sweeps all the mass that it finds in its path. The rest of the CS remains unchanged. This is supported by the large imbalance between P_m and the plasma pressure, which suggests that a shock structure would form in this interface.
- The pressure in front of the thin sheet is disregarded in the momentum equation.
- The starting time for this movement will be assumed to be equal to t_0 and the description will be valid until the thin sheet reaches $r_a + \delta$.

Under the mentioned hypotheses, the outer radius $r$of the initial CS satisfies

$$P_m 2\pi\, r d_a = \frac{\mu_0 I^2}{4\pi r} d_a = \frac{d}{dt}\left[m_D n_0 d_a \left(r^2 - r_a^2\right)\frac{dr}{dt}\right], \tag{3}$$

where, defining $C = \mu_0/4\pi^2 m_D n_0 r_a^4$, m_D is the deuteron mass and $x = r/r_a$ becomes

$$C I(t)^2 = x\frac{d}{dt}\left[(x^2-1)\frac{dx}{dt}\right]. \tag{4}$$

Equation (4) can be numerically integrated using measured values of $I(t)$ in any device, to obtain $x(t)$ in the range $1 < x < (r_a + \delta)/r_a$. The time needed for x reaching the upper limit of this interval is the time at which pictures of the CS would show the start of lift-off motions.

Taking into account the fact that the duration of the initial stage is much shorter than the quarter period of the discharge current, $I(t)$can be approached as

$$I(t) \cong \left(\frac{V_0}{L_0}\right) t. \tag{5}$$

Combining equations (4) and (5) and defining the reference time scale (i.e. $\tau = t/t_r$)

$$t_r = \left(\frac{4\pi^2 m_D n_0}{\mu_0}\right)^{1/4} \left(\frac{L_0}{V_0}\right)^{1/2} r_a \tag{6}$$

leads to the following dimensionless lift-off equation:

$$\tau^2 = x\frac{d}{d\tau}\left[(x^2-1)\frac{dx}{d\tau}\right], \tag{7}$$

with the initial conditions $x(0) = 1$, $dx/d\tau(0) = 0$.

A solution of equation (7) was obtained with the FORTRAN LSODE package (Hindmarsh 1983) and is given as a solid line in figure 3. The solution is dimensionless, and therefore it is valid for the initial stage of any specific PF device. The graphic shows the dimensionless time required to reach the external edge of an initial dimensionless plasma width δ/r_a. Expanding $x(\tau)$ in Taylor series (i.e. $x \approx c_0 + c_1\tau + c_2\tau^2 + \cdots$) and replacing in equation (7), the firsts coefficients of the expansion can be determined from a system of linear equations and the following approximate function can be obtained:

$$x - 1 \approx \frac{1}{\sqrt{12}}\tau^2 - \frac{11}{360}\tau^4, \tag{8}$$

which is shown as a dashed curve in figure 3.

The predictions of the τ values satisfying $x - 1 = \delta/r_a$ (lift-off condition) obtained from equation (8) can be compared against experimental data in any device. For the device used in the present study ($V_0 = 30$ kV, $L_0 = 40$ nH, $r_a = 2.3$ cm), the reference time is given by

$$t_r \approx 200 p_0^{1/4}\ \mathrm{ns/mbar}^{1/4} \tag{9}$$

and the outward dimensionless CS boundary $(r_a + \delta)/r_a$ is about 1.17 ($\delta \approx 4$ mm). Hence, the lift-off time is given by $\tau_l(x = 1.17) \approx 0.85$, resulting in

$$t_l(\mathrm{ns}) \approx 170\ \ [p_0(\mathrm{mbar})]^{1/4}. \tag{10}$$

Furthermore, the speed of the expanding thin sheet is $\mathrm{d}r/\mathrm{d}t = (r_a/t_r)\mathrm{d}x/\mathrm{d}\tau$. In our device this speed is given by $7.4\times10^6 \mathrm{d}x/\mathrm{d}\tau\, /[p_0(\mathrm{mbar})]^{1/4}$ m s^{-1}. Note that this velocity is independent of r_a. Hence for $\mathrm{d}x/\mathrm{d}\tau$ values of 0.001 (already attained at $\tau > 0.001$, as can be seen on deriving equation (8)) this speed is much larger than the sound speed in the CS. It is worth noting that this magnitude roughly applies to any device, since it is determined only by $(V_0/L_0)^{1/2}$, which changes very little in PF devices. This fact substantiates the notion that in PF devices the CS movement generates right from the very beginning a very strong shock front, such that the energy source for ionization and heating is the electromechanical work done by the magnetic piston instead of Joule heating.

Unfortunately no visual information of the CS movements is available from the GN1 device. However, visual information is available for a similar device discharging in hydrogen (Krompholz *et al* 1980). Using the corresponding parameters ($V_0 = 20$ kV, $L_0 = 90$ nH, $r_a = 2$ cm, p_0 (H_2) = 3 mbar, $\delta \approx 5$ mm), the lift-off time predicted by the present model is 290 ns, which agrees well with the reported value (300 ns).

Gourlan *et al* (1979) used magnetic probes in a 1 MJ PF facility, which can also be used to calculate the lift-off time. The parameters of this device were $r_a = 8.8$ cm, $V_0 = 20$ kV, $L_0 = 16$ nH, $p_0 = 4$ mbar, and assuming $\delta \approx 1.5$ cm, the predicted lift-off time is about 1 μs, in good agreement with that found experimentally.

4. Lift-off inductance dynamics

The present lift-off model can be applied to assess the temporal evolution of the gun inductance associated with the initial movement of the CS. The diffusion time of the current density j in the initial CS can be estimated as $\mu_0\delta^2/\eta(t_0)$ and it is about 8 ns at 1 mbar, much smaller than the estimated lift-off time. During the radial expansion of the thin sheet the resistivity of the unperturbed portion of the CS should fall, but the diffusion length $(\delta - r)$ also diminishes, so that it is reasonable to assume that j redistributes instantaneously within the cross section of the unperturbed CS during the lift-off stage. Therefore, the lift-off current density inside the CS can be calculated as

$$j(r, t) = \frac{I}{\pi\left[(r_a + \delta)^2 - r^2\right]}. \tag{11}$$

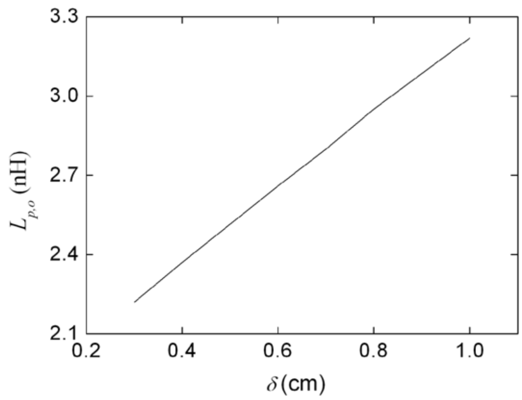

Figure 4. Theoretical initial gun inductance in the device GN1 as a function of δ.

The corresponding magnetic field B at any radial position r' between the anode and the outer radius of the CS is given by

$$B(r',t) = \begin{cases} \left(\dfrac{\mu_0 I(t)}{2\pi\, r'}\right) & \text{if} \quad a < r' < r(t) \\ \dfrac{\mu_0 I(t)}{2\pi\, r'}\left[1 - \dfrac{r'^2 - r^2}{(r_\mathrm{a}+\delta)^2 - r^2}\right] & \text{if} \quad r(t) < r' < r_\mathrm{a} + \delta \end{cases} \tag{12}$$

where a is the anode radius. Considering that

$$L_\mathrm{p}(t) = \frac{d_\mathrm{a}}{I(t)} \int_a^{r_\mathrm{a}+\delta} B(r',t)\mathrm{d}r', \tag{13}$$

the temporal evolution of the gun inductance during the lift-off stage can be estimated as

$$L_\mathrm{p}(t) = \frac{\mu_o d_\mathrm{a}}{2\pi}\left[\ln\left(\frac{r_\mathrm{a}+\delta}{a}\right) - 0.5 + \frac{\ln\left(\dfrac{1+\delta/r_\mathrm{a}}{x(t)}\right)}{\left(\dfrac{1+\delta/r_\mathrm{a}}{x(t)}\right)^2 - 1}\right]. \tag{14}$$

This estimation neglects for simplicity movements of the frontal part of the plasma sheet (the axial length is taken as constant), so it yields lower estimates for L_p. The inclusion of frontal movements would require coupled 2D equations, leading to the well-known bullet-shaped CS profile of later stages; however, 2D approaches are beyond the scope of this work.

It can be seen that L_p depends on geometrical parameters of the device (d_a, r_a, a) and on the plasma width δ when the CS starts moving ($x = 1$). Figure 4 shows the initial expected values of L_p for the GN1 geometry at different δ values. Note that considerable variations in δ produce only moderate changes in L_p, so that the determination of the initial L_p value in each experimental condition needs careful examination, which will be discussed later.

Equation (14) can be compared against experimental measurements of the gun inductance. Using the voltage and current derivative signals, the inductance dynamics during discharges in GN1 was indirectly calculated (Bruzzone *et al* 2006b). Figures 5 to 7 show the temporal evolution of L_p (solid lines) at the initial stage of discharges at 1 mbar, 3 mbar and 5 mbar, respectively. The oscillations observed in the experimental curves are due to the transmission lines connecting the capacitor bank to the electrodes (Bruzzone *et al* 1990). The corresponding theoretical predictions based on equation (14) (dashed lines) are compared in each graphic.

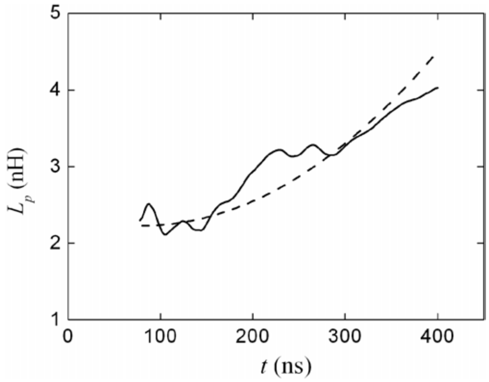

Figure 5. Temporal evolution of L_{p} during the lift-off stage (1 mbar). The solid line is the experimental determination, the dashed line corresponds to the present model.

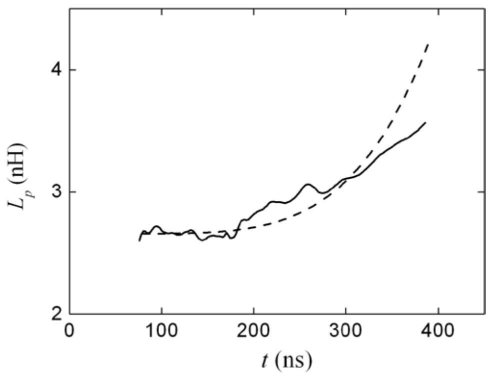

Figure 6. Temporal evolution of L_{p} during the lift-off stage (3 mbar). The solid line is the experimental determination, the dashed line corresponds to the present model.

It can be seen that in all these cases the model fits reasonably well the experimental data, at least up to the estimated t_{l} values measured with this method ($\approx$170 ns for 1 mbar, 250 ns for 3 mbar and 370 ns for 5 mbar). The analysis of all the data sets (some 60 shots) between 1 and 6 mbar also gives good agreement.

The parameter δ of the theoretical curves shown in figures 5 to 7 was determined by fitting the initial value of L_{p} (at typical t_0 values $\sim$100 ns). Fortunately, the method of inductance evaluation used in this work has enough sensitivity to detect relatively small variations in this initial value. Through these values and the plot in figure 4, the corresponding δ values found in this experimental run are 0.4 cm at 1 and 2 mbar, 0.6 cm at 3 mbar and 0.8 cm at 4 mbar. At 5 mbar, shot to shot variations of δ between 0.8 and 1 cm were found and between 1 and 1.2 cm at 6 mbar. The physical explanation for this behaviour would require the study of the breakdown mechanism and the associated processes (avalanche formations, streamers, merging of streamers, etc), which is beyond the scope of the present work.

5. Conclusions

A model of the lift-off of the CS during the initial stage of PF discharges was presented. In spite of its simplicity, the model was contrasted against experimental measurements on low energy

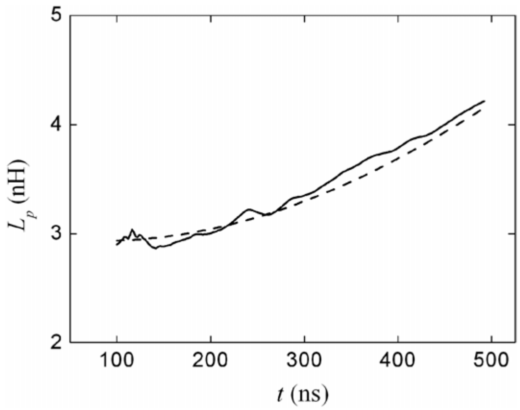

Figure 7. Temporal evolution of L_p during the lift-off stage (5 mbar). The solid line is the experimental determination, the dashed line corresponds to the present model.

devices, showing good agreement. It was found that the lift-off thickness of the CS increases with the filling pressure. The model hypotheses are sufficiently general so that they can be applied to any PF device. The results presented in the analysis imply that the descriptions of CS kinematics through snowplough models do not require lift-off corrections, provided that the appropriate initial current time (t_0) is used in the calculations.

References

Brown S C 1967 *Basic Data of Plasma Physics, 1966* (New York: MIT Press)

Bruzzone H, Kelly H and Moreno C 1989 On the effect of finite closure time of switches in fast transient electrical circuits *Am. J. Phys.* **57** 63–8

Bruzzone H, Kelly H and Moreno C 1990 The effect of transmission lines and switching action on the electrical signals in a powerful capacitive discharge *IEEE Trans. Plasma Sci.* **PS-18** 689–96

Bruzzone H and Grondona D 1997 Magnetic probe measurements of the initial phase in a plasma focus device *Plasma Phys. Control. Fusion* **39** 1315–26

Bruzzone H and Acuña H 2006a The breakdown stage in long laser tubes and plasma focus devices *Plasma Sources Sci. Technol.* **15** 489–94

Bruzzone H, Acuña H, Barbaglia M and Clausse A 2006b A simple plasma diagnostic based on processing the electrical signals from coaxial discharges *Plasma Phys. Control. Fusion* **48** 609–20

Casanova F, Moreno C and Clausse A 2005 Finite-elements numerical model of the current-sheet movement and shaping in coaxial discharges *Plasma Phys. Control. Fusion* **47** 1239–50

González J, Florido P, Bruzzone H and Clausse A 2004 A lumped parameter model of plasma focus *IEEE Trans. Plasma Sci.* **32** 1383–91

Gourlan C, Kroegler H, Maisonnier C, Rager J, Robouch B, Bertalot L and Gentilini A 1979 *Nucl. Fusion Suppl.* II **2** 123–6

Hindmarsh A C 1983 ODEPACK: a systematized collection of ODE solvers *Scientific Computing* ed R Stepleman *et al* 55–64

Huba J D 2006 *Revised NRL Plasma Formulary*, Naval Research Laboratory, Washington

Krompholz H, Neff W, Ruhl F, Schonbach K and Herziger G 1980 Formation of the plasma layer in a Plasma Focus device *Phys. Lett.* A **77** 246–8

Moreno J, Silva P and Soto L 2003 Optical observations of the plasma motion in a fast plasma focus operating at 50 J *Plasma Sources Sci. Technol.* **12** 39–45

Oppenlander T 1978 Measurement of magnetic field and current density distribution in the Frascati 1 MJ Plasma Focus device *CNEN Internal Report 78.6*